Theoretical analysis of transcription process with polymerase stalling

Jingwei Li and Yunxin Zhang*

Laboratory of Mathematics for Nonlinear Science, Shanghai Key Laboratory for Contemporary Applied Mathematics, Centre for Computational Systems Biology, School of Mathematical Sciences, Fudan University, Shanghai 200433, China

(Received 6 February 2015; revised manuscript received 16 April 2015; published 28 May 2015)

Experimental evidence shows that in gene transcription RNA polymerase has the possibility to be stalled at a certain position of the transcription template. This may be due to the template damage or protein barriers. Once stalled, polymerase may backtrack along the template to the previous nucleotide to wait for the repair of the damaged site, simply bypass the barrier or damaged site and consequently synthesize an incorrect messenger RNA, or degrade and detach from the template. Thus, the *effective* transcription rate (the rate to synthesize correct product mRNA) and the transcription *effectiveness* (the ratio of the effective transcription rate to the effective transcription initiation rate) are both influenced by polymerase stalling events. So far, no theoretical model has been given to discuss the gene transcription process including polymerase stalling. In this study, based on the totally asymmetric simple exclusion process, the transcription process including polymerase stalling is analyzed theoretically. The dependence of the effective transcription rate, effective transcription initiation rate, and transcription effectiveness on the transcription initiation rate, termination rate, as well as the backtracking rate, bypass rate, and detachment (degradation) rate when stalling, are discussed in detail. The results showed that backtracking restart after polymerase stalling is an ideal mechanism to increase both the effective transcription rate and the transcription effectiveness. Without backtracking, detachment of stalled polymerase can also help to increase the effective transcription rate and transcription effectiveness. Generally, the increase of the bypass rate of the stalled polymerase will lead to the decrease of the effective transcription rate and transcription effectiveness. However, when both detachment rate and backtracking rate of the stalled polymerase vanish, the effective transcription rate may also be increased by the bypass mechanism.

DOI: 10.1103/PhysRevE.91.052713 PACS number(s): 87.16.aj, 87.15.rp, 05.70.−a, 87.16.Uv

I. INTRODUCTION

Replication, transcription, and translation are three basic processes in cells. Before cell division, a cell replicates its DNA with the help of DNA polymerase. Using DNA as a template, messenger RNA (mRNA) is synthesized by RNA polymerase (RNAP) during the so-called transcription process. Then using mRNA as a template, the peptide chain is synthesized by ribosomes during the translation process and proteins are then obtained by the folding of peptide chains. Roughly speaking, each of the three processes includes three subprocesses: initiation, elongation, and termination. The product is synthesized by polymerase during its forward motion along template in the elongation process.

In the field of theoretical studies, the transcription process is usually described by the totally asymmetric simple exclusion processes (TASEPs) (see [1–7]), in which RNAP is regarded as a point particle, and the template DNA is regarded as a one-dimensional lattice with lattice sites corresponding to the nucleotides in DNA. The transcription initiation corresponds to the binding of RNAP to the first lattice site, where the first site can be regarded as a combination of the promoter and the transcription start site. The transcription termination corresponds to the leaving of particles from the last site of the lattice. The elongation of transcription is described by the forward hopping of particle in the main body of the lattice. The totally asymmetric exclusion means that the polymerase at site i can only hop forward to site $i+1$ provided that it is not occupied. In TASEP, the forward hopping rates of particles at any site i of the lattice are always assumed to be the same and simply normalized to be 1. It implies that RNAP will move along DNA template with constant speed until the termination site. However, several experimental observations found that the regular elongation procedure may be interrupted, with RNAP stalled at a certain nucleotide. The stalling of RNAP may be caused by several reasons. Structural aberrations of the template can trigger a stalling of polymerase [8–10]. Polymerase may also be stalled from the depletion of building blocks nucleoside triphosphate [11] or from the template damage [12–17]. Meanwhile, the damage or incorrect assembling of polymerase itself may also lead to stalling [18].

In both prokaryotic and eukaryotic cells, there are several mechanisms which are usually employed by polymerase to solve the stalling problem. If the stalling is caused by template damage, polymerase may backtrack along the template to the previous site and wait for the repair of the damaged site [19–26]. The synthesis of mRNA is able to restart after the repair. Alternatively, the stalled polymerase may simply bypass the damaged site and continue the transcription process from the downstream site and finally end the transcription at the termination site with an incorrect product [17,20–22,27,28]. Meanwhile, if a prolonged stalling occurs, the polymerase may be degraded as a mechanism of last resort [29]. By the way, in the translation process, recent experiments have also found that the template (mRNA) can degrade when the translocation of ribosomes is stalled [30–33].

The polymerase stalling as well as the possible mechanisms employed by the stalled polymerase will affect the overall transcription rate and efficiency and consequently have influence on the strength of gene expression. Thus, the related properties of transcription are not only determined by the initiation rate

*xyz@fudan.edu.cn

and termination rate as implied in the usual TASEP model, but also influenced by the polymerase stalling and corresponding mechanisms used to overcome the stalling problem. Although there are various kinds of generalizations of the TASEP model, no one can be used directly to describe the gene transcription process with polymerase stalling.

In this study, a modified TASEP model is presented to describe the gene transcription process including polymerase stalling. For simplicity, this study assumes that there is only one nucleotide in the transcription template at which polymerase may be stalled, and the position of this nucleotide is unchanged for any polymerase. This nucleotide may be damaged or bound by protein complexes, or there is one special secondary structure around it. The stalled polymerase may backtrack along the template to the previous binding site to wait for the repair of the damaged site (or clearance of the barrier), simply bypass this nucleotide and synthesize an incorrect mRNA product, or degrade and detach from the transcription template; see Fig. 1. This study mainly focuses on four rates: the *effective* initiation rate, the effective transcription rate, the *bypass* transcription rate, and the transcription *effectiveness* (see the first paragraph of Sec. III for detailed definitions of them). Numerical calculations of our modified TASEP model show that the effective transcription rate may be enlarged by increasing the backtracking rate, detachment rate, and bypass rate of the stalled polymerase. Even the transcription effectiveness may be increased with the backtracking and detachment rates. Generally, backtracking is one ideal mechanism to solve the polymerase stalling problem. Without backtracking, detachment and bypass are also good mechanisms to increase the effective transcription rate. However, bypass or detachment mechanism cannot be generally replaced by the backtracking mechanism, especially when the rate of transcription restart after backtracking is relatively low.

This study is organized as follows. The modified TASEP model describing the transcription process including polymerase stalling is presented in the next section, and then the results obtained by this model are given in Sec. III. Finally, concluding remarks are presented in the last section.

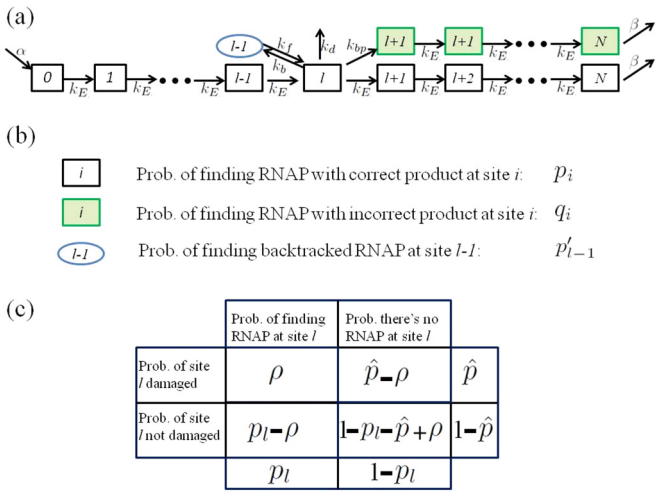

FIG. 1. (Color online) (a) Modified TASEP model to describe gene transcription process with possible polymerase stalling at site l. Transcription starts with polymerase binding to the first site 0 (with the rate denoted by α) and terminated at the last site N with the rate denoted by β. At site l, the forward translocation of polymerase may be stalled. There are three mechanisms for a stalled polymerase to leave the damaged site l: backtracking to site $l-1$ with rate k_b, degrading and detaching from the template with rate k_d, or just bypassing the site l with rate k_{bp} and continuing its translocation along the template (but the mRNA synthesized by it is incorrect and will degrade soon). During transcription elongation period, the forward stepping rate of polymerase is denoted by k_E, which is assumed to be the same throughout the transcription, for polymerases in whatever states (correct or incorrect). (b) Notations for probabilities of finding polymerase at corresponding states, with correctly transcribed mRNA (p_i), incorrectly transcribed mRNA (q_i), and backtracked polymerase at site $l-1$ (p'_{l-1}). (c) Notations for probabilities related to site l, which may be damaged with or without polymerase binding.

II. MODIFIED TASEP MODEL FOR GENE TRANSCRIPTION WITH POLYMERASE STALLING

The model used in this study can be regarded as a modification of the usual TASEP, which is schematically depicted in Fig. 1, where the length of the gene is assumed to be $N+1$ and each lattice site stands for one nucleotide or nucleotide group (which means this model is obtained by coarse grain). The TASEP model has been used to analyze transcription and translation for many years [34–36]. For simplicity, the length of polymerase is not explicitly considered in this study.

The transcription begins with RNAP binding to lattice site 0 (corresponding to the promoter upstream the gene) with rate α, which depends on the concentration of free polymerase in environment, the binding rate of transcription factors, and the nucleotide sequence of promoter [37]. The transcription is ended by polymerase leaving from lattice site N, with the corresponding rate denoted by β. This study assumes that only lattice site l may be damaged (or occupied by a protein complex). The rate constant that site l becomes damaged is denoted by $k_{\hat{p}d}$. If the damaged site l is not occupied by a polymerase, then it can be repaired with rate $k_{\hat{p}r}$. See Eq. (3) for the dynamics of probability that site l is damaged. If the site l is damaged, polymerase on it may bypass it directly (with no transcription) and continue its forward translocation along the template and finally leave from the stop site N, but the product (i.e., mRNA) synthesized by it will be incorrect and will degrade soon [38]. In this study, the probability that there is a polymerase with a *correct* semifinished product at site i (for $0 \leqslant i \leqslant N$) is denoted by p_i, and the probability that there is a polymerase with an *incorrect* semifinished product at site i (for $l+1 \leqslant i \leqslant N$) is denoted by q_i. A polymerase at site i (for $i \neq l$) will move to site $i+1$ with rate k_E provided site $i+1$ is unoccupied.

If the site l is damaged, polymerase at this site will be stalled. Experiments found that there are three possible mechanisms for the stalled polymerase to leave the damaged site l. (1) The polymerase may backtrack to the previous site $l-1$ with rate k_b provided the site $l-1$ is not occupied. Generally, there are other causes of polymerase backtracking besides a damaged site, such as nucleotide misincorporation which comprises a significant role of backtracking. However, for simplicity, we include them implicitly in the elongation

rate k_E in this study. After the repair of site l, the backtracked polymerase will return to site l with rate k_f. The probability of finding a backtracked polymerase at site $l-1$ is denoted by p'_{l-1}. See Eq. (5) for the dynamics of probability p'_{l-1}. (2) The polymerase may bypass the damaged site l with rate k_{bp} and continue its transcription from the downstream site $l+1$. (3) The polymerase may degrade with rate k_d and detach from the transcription template. Note that the genetic information coded in damaged site l cannot be transcribed. Therefore, the mRNA synthesized by a polymerase which has bypassed the damaged site l is nonfunctional and will degrade soon [38]. Meanwhile, the damaged site l cannot be repaired if there is a polymerase binding on it. Thus, if $k_b = 0$, $k_{bp} = 0$, and $k_d = 0$, the polymerase will be stalled at the damaged site l forever. So bypass, degradation, and backtracking are three important mechanisms for cells to continue the transcription process. Otherwise, the template will be totally blocked.

This study assumes that each site i can only be occupied by one polymerase. If there is one backtracked polymerase at site $l-1$, the site l will be unoccupied. This is because that the backtracked polymerase at site $l-1$ is from site l. In the following, the probability of finding a polymerase at damaged site l is denoted by ρ. For the model depicted in Fig. 1, the probabilities p_i are governed by the following equations:

$$\begin{aligned}
dp_0/dt &= \alpha(1-p_0) - k_E p_0(1-p_1),\\
dp_i/dt &= k_E p_{i-1}(1-p_i) - k_E p_i(1-p_{i+1}), \quad \text{for } 1 \leqslant i \leqslant l-3,\\
dp_{l-2}/dt &= k_E p_{l-3}(1-p_{l-2}) - k_E p_{l-2}(1-p_{l-1}-p'_{l-1}),\\
dp_{l-1}/dt &= k_E p_{l-2}(1-p_{l-1}-p'_{l-1}) - k_E p_{l-1}(1-p_l),\\
dp_l/dt &= k_E p_{l-1}(1-p_l) - k_E(p_l-\rho)(1-p_{l+1}-q_{l+1}) + k_f(1-\hat{p})p'_{l-1}\\
&\quad -k_b\rho(1-p_{l-1}-p'_{l-1}) - k_{bp}\rho(1-p_{l+1}-q_{l+1}) - k_d\rho,\\
dp_{l+1}/dt &= k_E(p_l-\rho)(1-p_{l+1}-q_{l+1}) - k_E p_{l+1}(1-p_{l+2}-q_{l+2}),\\
dp_i/dt &= k_E p_{i-1}(1-p_i-q_i) - k_E p_i(1-p_{i+1}-q_{i+1}), \quad \text{for } l+2 \leqslant i \leqslant N-1,\\
dp_N/dt &= k_E p_{N-1}(1-p_N-q_N) - \beta p_N.
\end{aligned} \tag{1}$$

Where the equations for $0 \leqslant i \leqslant l-3$ and $l+2 \leqslant i \leqslant N$ can be obtained similarly as in the usual TASEP model. The total probability of finding polymerase at site $l-1$ is $p_{l-1} + p'_{l-1}$, where p_{l-1} is the probability of polymerase which comes from site $l-2$ and p'_{l-1} is the probability of polymerase which is backtracked to site $l-1$ from the damaged site l. The probability flux from site $l-2$ to site $l-1$, which is related to the governing equations of probabilities p_{l-2} and p_{l-1}, is $k_E p_{l-2}(1-p_{l-1}-p'_{l-1})$. In the governing equation of probability p_l, the first term is the flux from site $l-1$ to site l. The second term is the flux from undamaged site l to site $l+1$, where $p_l - \rho$ is the probability that there is a polymerase at site l and site l is not damaged. The third term is the return flux from site $l-1$ to site l of the backtracked polymerase, where $1-\hat{p}$ is the probability that the damaged site l has been repaired. The fourth term is the backtracking flux. The fifth term is the bypass flux, and the final term is the detachment flux. The governing equation for probability p_{l+1} can be obtained similarly.

Meanwhile, the probabilities q_i satisfy [see Fig. 1(b) for the meanings of probabilities q_i]

$$\begin{aligned}
dq_{l+1}/dt &= k_{bp}\rho(1-p_{l+1}-q_{l+1})\\
&\quad - k_E q_{l+1}(1-p_{l+2}-q_{l+2}),\\
dq_i/dt &= k_E q_{i-1}(1-p_i-q_i) - k_E q_i(1-p_{i+1}-q_{i+1}),\\
&\quad \text{for } l+2 \leqslant i \leqslant N-1,\\
dq_N/dt &= k_E q_{N-1}(1-p_N-q_N) - \beta q_N,
\end{aligned} \tag{2}$$

where the probability $\hat{p}$ that site l is damaged satisfies

$$d\hat{p}/dt = k_{\hat{p}d}(1-\hat{p}) - k_{\hat{p}r}(\hat{p}-\rho), \tag{3}$$

in which the second term is from the assumption that only the unoccupied site l can be repaired. The probability ρ that there is a polymerase at the damaged site l can be obtained as

$$\begin{aligned}
d\rho/dt &= k_{\hat{p}d}(p_l-\rho) + k_E p_{l-1}(\hat{p}-\rho)\\
&\quad - k_{bp}\rho(1-q_{l+1}-p_{l+1}) - k_d\rho\\
&\quad - k_b\rho(1-p'_{l-1}-p_{l-1}),
\end{aligned} \tag{4}$$

where the first term is the flux of the probability that the occupied site l becomes damaged. The second term is the flux of probability that a polymerase translocates from site $l-1$ to the unoccupied but damaged site l. The last three terms are bypass flux, detachment flux, and backtracking flux, respectively. Finally, the probability p'_{l-1} that there is a backtracked polymerase at site $l-1$ satisfies

$$dp'_{l-1}/dt = k_b\rho(1-p_{l-1}-p'_{l-1}) - k_f(1-\hat{p})p'_{l-1}, \tag{5}$$

where the first term is the backtracking probability flux of the stalled polymerase from the damaged site l to its upstream site $l-1$, and the second term is the return probability flux of the backtracked polymerase. For convenience, meanings of probabilities p_l, $\hat{p}$, ρ are displayed in Fig. 1(c). The total probability of finding a polymerase at site i, no matter whether it is with a correctly synthesized mRNA or an incorrect mRNA, is denoted by P_i, or mathematically,

$$P_i = \begin{cases} p_i, & \text{for} \quad 0 \leqslant i \leqslant l-2 \text{ or } i = l,\\ p_{l-1} + p'_{l-1}, & \text{for} \quad i = l-1,\\ p_i + q_i, & \text{for} \quad l+1 \leqslant i \leqslant N. \end{cases} \tag{6}$$

III. RESULTS

All results of this study are based on the steady state solution of Eqs. (1)–(5), which are obtained by numerical calculations performed in software MATLAB. First, we defined the effective

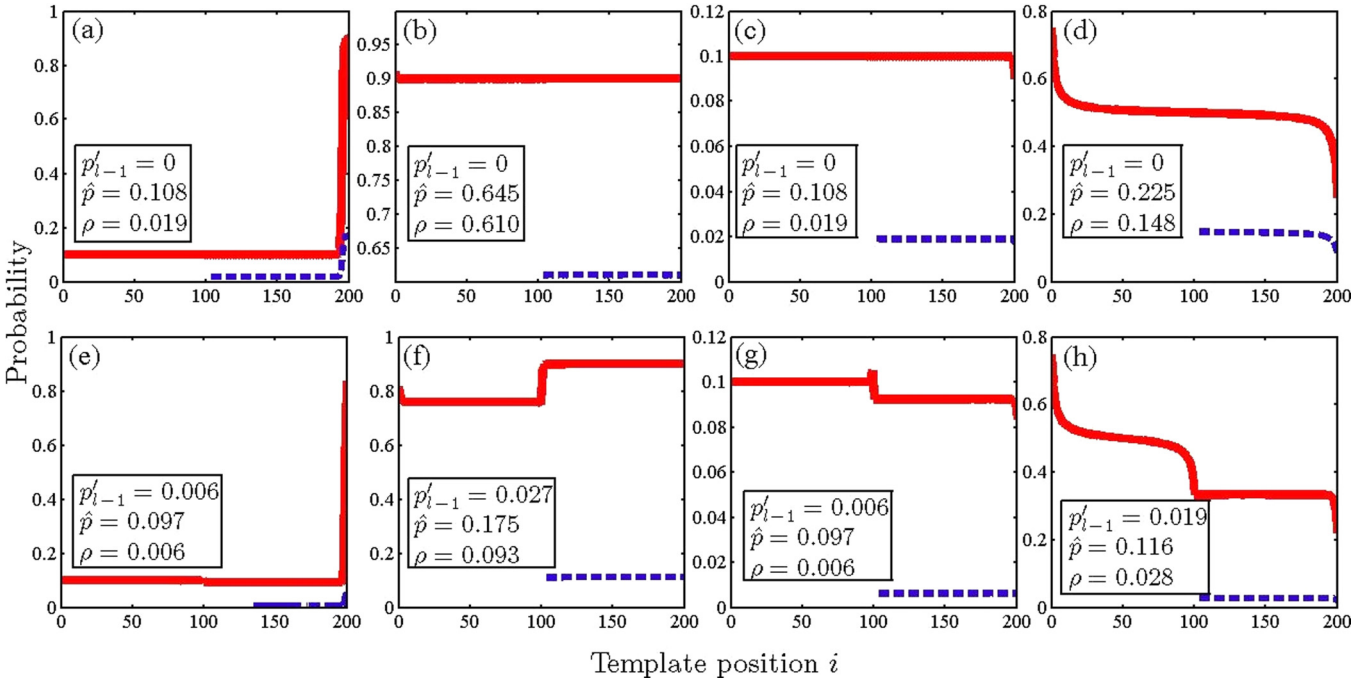

FIG. 2. (Color online) Typical examples of probabilities P_i (solid lines), q_i (dashed lines), p'_{l-1}, $\hat{p}$, and ρ (given in legends) along the gene, which are obtained from Eqs. (1)–(6) with gene length $N = 100$. Panels (a)–(d) are for simplified cases where detachment and backtracking of polymerase from damaged site l are not allowed, i.e., $k_b = k_d = 0$, while panels (e)–(h) are for cases with nonzero detachment rate and backtracking rate. Except the values of k_b and k_d, other parameter values used in (a)–(d) are the same as the ones used in (e)–(h) respectively; see Table I. Panels (a), (c), (e), (g) are examples of the low probability density case with probability less than 0.5, (b) and (f) are examples of high density case with probability larger than 0.5, and (d) and (h) are examples of maximal flux case. The sharp decrease of probability P_i after site $l = 100$ is due to the polymerase detachment from site l. For the meanings of probability notations, see Fig. 1.

initiation rate by $\alpha_{\text{eff}} := \alpha(1 - p_0)$. It is different from the initiation rate α and is called effective because it reflects the rate at which a polymerase meets the empty initiation site of the template and starts a transcription (meeting an occupied initiation site will not start a transcription, thereby not being effective). Second, we define the effective transcription rate as $\beta_{\text{eff}} := \beta p_N$. In fact, it is the rate of synthesizing correct products. Third, we define the bypass transcription rate as $\beta_{bp} = \beta q_N$. It stands for the rate of synthesizing incorrect products. Finally, we define the transcription effectiveness as $r := \beta_{\text{eff}}/\alpha_{\text{eff}}$. One may ask why such an odd value should be discussed. As we all know, polymerase is an important resource for a cell. Thus, a larger r means not only saving more energy, but also saving more polymerase since a transcription ended with an incorrect production will kidnap polymerase for a long time. This study mainly focuses on relationships between effective rates α_{eff}, β_{eff}, and β_{bp}, effectiveness r, and related model parameters and tries to show that how the transcription process is influenced by the three mechanisms (backtracking restart, bypassing, and degradation) employed by stalled polymerase.

A. Typical examples of polymerase probabilities along the transcription template

To illustrate the properties of gene transcription with possible stalling of polymerase at a given position, typical examples of related probabilities, obtained by the modified TASEP model, are plotted in Fig. 2, where Figs. 2(a)–2(d) are for the cases where $k_b = k_d = 0$, i.e., the backtracking rate to the upstream site $l - 1$ and detachment rate from site l for stalled polymerase at site l vanish. For these special cases, the total probability P_i of finding polymerase at site i may have three different phases, low density phase [Figs. 2(a) and 2(c)], high density phase [Fig. 2(b)], and maximal flux phase [Fig. 2(d)], where the probability flux is defined by $J_i = K_E P_i(1 - P_i)$, which reaches its maximal value 1/4 when $P_i \equiv 1/2$. Meanwhile, boundary layers may exist at one or both of the two boundaries, $i = 0$ and $i = N$. These properties are similar to the ones of usual TASEP models, and the probability and corresponding flux are fully determined by the transcription initiation rate α and the transcription termination rate β; see [3,4]. For general cases with nonzero values of backtracking rate k_b and detachment rate k_d, the plots in Figs. 2(e)–2(h) show that the probability P_i has a sharp change at the site l. For the sake of comparison, except k_b and k_d, other parameter values used in Figs. 2(e)–2(h) are the same as the ones used in Figs. 2(a)–2(d), respectively; see Table I. Since polymerase at damaged site l may degrade and detach from the transcription template, different with the ones plotted in Figs. 2(a)–2(d), the probability flux $J_i = K_E P_i(1 - P_i)$ for the general cases is not conversed along the template. Meanwhile, since polymerase can only detach or backtrack from the damaged site l, the flux J_i is conversed both in the region between site $i = 0$ and site $i = l - 1$ and in the region between sites $i = l + 1$ and $i = N$. Because of the detachment, the probability flux will be reduced after site l. This means that for the cases of low density phase and

TABLE I. Parameter values used in the calculations of Fig. 2.

Figure	N	k_E	l	α	β	k_b	k_{bp}	k_d	k_f	$k_{\hat{p}d}$	$k_{\hat{p}r}$
2(a)	200	1	100	0.1	0.1	0	1	0	1	0.1	1
2(b)	200	1	100	1	0.1	0	1	0	1	0.1	1
2(c)	200	1	100	0.1	1	0	1	0	1	0.1	1
2(d)	200	1	100	1	1	0	1	0	1	0.1	1
2(e)	200	1	100	0.1	0.1	1	1	1	1	0.1	1
2(f)	200	1	100	1	0.1	1	1	1	1	0.1	1
2(g)	200	1	100	0.1	1	1	1	1	1	0.1	1
2(h)	200	1	100	1	1	1	1	1	1	0.1	1

maximal flux phase, the probability P_i will be reduced after site l [see Figs. 2(e), 2(g), and 2(h)], while for the cases of high density phase, P_i will be increased [see Fig. 2(f)]. Due to the backtracking of polymerase from damaged site l, the total probability of finding polymerase at site $l-1$, P_{l-1}, may be higher than those of other sites; see Fig. 2(g).

The plots in Figs. 2(a)–2(d) imply that, without polymerase detachment, the total transcription rate may not be reduced by the site damage. However, the effective (or *correct*) transcription rate, i.e., the rate to synthesize correct mRNA, will be reduced. Given the nonzero bypass rate k_{bp}, some products are incorrect and will degrade rapidly. With additional detachment of polymerase from the damaged site l, for general cases, the effective transcription rate is less than the effective transcription initial rate; see Figs. 2(e)–2(h). In this study, the effective transcription initial rate is defined as $\alpha_{\text{eff}} := \alpha(1-p_0)$, the effective transcription rate is defined as $\beta_{\text{eff}} := \beta p_N$, and the bypass transcription rate is defined as $\beta_{bp} := \beta q_N$. In the following, the parameter dependent properties of α_{eff}, β_{eff}, β_{bp}, and the ratio $r := \beta_{\text{eff}}/\alpha_{\text{eff}}$ are discussed in detail. The ratio r is one reasonable index to describe the effectiveness of transcription including polymerase stalling.

B. Properties of effective rates α_{eff}, β_{eff}, and β_{bp} and effectiveness r

The plots in Fig. 3 show that with nonzero detachment rate k_d, all the effective rates α_{eff}, β_{eff}, and β_{bp} decrease with the position l of damaged site, but the transcription effectiveness r increases with l (see the lines in Fig. 3 with marker "$\circ$"). Given that polymerase can only detach from the damaged site l, if the location l of damaged nucleotide is far from the initiation site 0, then the polymerase density between sites 0 and l will be high and consequently the polymerase current along the gene will be low. Thus, the effective transcription initiation rate α_{eff} is decreased with l. Except from the damaged site l, polymerase cannot detach from the transcription template; therefore, a low effective initiation rate will lead to a low transcription rate. Thus, effective transcription rate β_{eff} and bypass transcription rate β_{bp} also decrease with the damaged position l. The increase of transcription effectiveness r with damaged position l implies that large values of damaged position l will be beneficial for cells to increase the transcription efficiency and save energy molecules. On the other hand, for nondetachment cases, i.e., $k_d = 0$ (see the lines in Fig. 3 with marker "$*$"), the effective initiation rate α_{eff} is independent of damaged position l, but the effective transcription rate β_{eff} increases

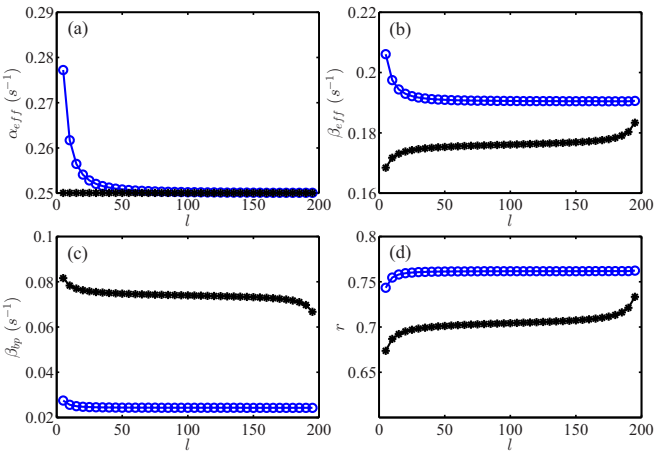

FIG. 3. (Color online) The effective transcription initiation rate $\alpha_{\text{eff}} := \alpha(1-p_0)$ (a), effective (or correct) transcription rate $\beta_{\text{eff}} := \beta p_N$ (b), bypass transcription rate $\beta_{bp} := \beta q_N$ (c), and the transcription effectiveness $r := \beta_{\text{eff}}/\alpha_{\text{eff}}$ (d) as functions of the position l of damaged site, which changes from 5 to 195 with an increment of 5. For other parameter values, see Table II. The only difference between the two lines in each figure is that, for the lines with marker "$*$", the detachment rate k_d is equal to zero, while for the lines with marker "$\circ$", the detachment rate k_d is nonzero.

with l. Thus, the transcription effectiveness $r = \beta_{\text{eff}}/\alpha_{\text{eff}}$ also increases with damaged position l. Therefore, for any case (with or without detachment of polymerase from the damaged site), large values of damaged position l will help to increase the transcription efficiency. The plots in Fig. 3 also show that, except for the cases where the damaged site of template is close to the transcription start site or termination site, α_{eff}, β_{eff}, β_{bp}, and r are not sensitive to the damaged position l.

Figure 4(a) shows that the effective transcription initiation rate α_{eff} increases with the initiation rate α and tends to

TABLE II. Parameter values used in the calculations of Figs. 3–10.

Figures	Label	N	k_E	l	α	β	k_b	k_{bp}	k_d	k_f	$k_{\hat{p}d}$	$k_{\hat{p}r}$
3(a), 3(b), 3(c), 3(d)	$\circ$	200	1		1	1	0	1	1	1	0.1	1
	$*$	200	1		1	1	0	1	0	1	0.1	1
4(a), 4(b), 4(c), 4(d)	$\circ$	200	1	100		0.1	0	1	1	1	0.1	1
	$*$	200	1	100		1	0	1	1	1	0.1	1
	-	200	1	100		0.1	0	1	0	1	0.1	1
5(a), 5(b), 5(c), 5(d)	$\circ$	200	1	100	1		1	1	0	1	0.1	1
	$*$	200	1	100	1		0	1	1	1	0.1	1
6(a), 6(b), 6(c), 6(d)	$\circ$	200	1	100	1	1		1	0	1	0.1	1
7(a), 7(b), 7(c), 7(d)	$\circ$	200	1	100	1	1	0		0	1	0.1	1
	$*$	200	1	100	1	1	1		0	1	0.1	1
	-	200	1	100	1	0.1	0		1	1	0.1	1
8(a), 8(b), 8(c), 8(d)	$\circ$	200	1	100	1	0.1	0	1		1	0.1	1
	$*$	200	1	100	1	0.1	1	1		1	0.1	1
	-	200	1	100	1	1	1	1		1	0.1	1
9(a), 9(b), 9(c), 9(d)	$\circ$	200	1	100	1	1	1	1	0		0.1	1
	$*$	200	1	100	1	0.1	1	1	1		0.1	1
10(a), 10(b), 10(c), 10(d)	$\circ$	200	1	100	1	1	1	1	0	1		1
	$*$	200	1	100	1	1	1	0	1	1		1
	-	200	1	100	1	0.1	0	1	1	1		1

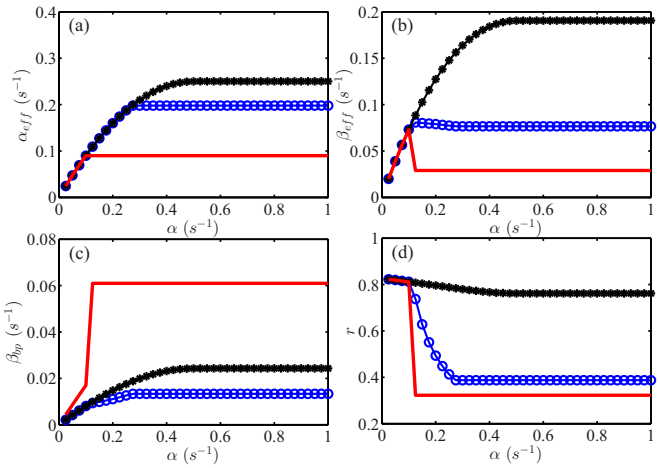

FIG. 4. (Color online) The effective transcription initiation rate α_{eff} (a), effective transcription rate β_{eff} (b), bypass transcription rate β_{bp} (c), and the effectiveness $r := \beta_{\text{eff}}/\alpha_{\text{eff}}$ (d) as functions of the transcription initiation rate α. In each figure, three typical examples are plotted. In calculations, the initiation rate α changes from 0.025 to 1 with an increment of 0.025, and other parameter values are listed in Table II. In contrast to the lines with marker "$\circ$", the thick solid lines are obtained with zero detachment rate, i.e., $k_d = 0$, while the lines with marker "$*$" are obtained with larger termination rate β. These plots show that $\alpha = 0.1$ is a critical value. When $\alpha \leqslant 0.1$, polymerase probabilities are in low value phase with right boundary layer, as well as large β_{eff} and small β_{bp}. On the other hand, when $\alpha > 0.1$, probabilities are in high value phase with left boundary layer, as well as small β_{eff} and large β_{bp}. The shifting of the boundary layer from right to left is the cause of the discontinuity at $\alpha = 0.1$.

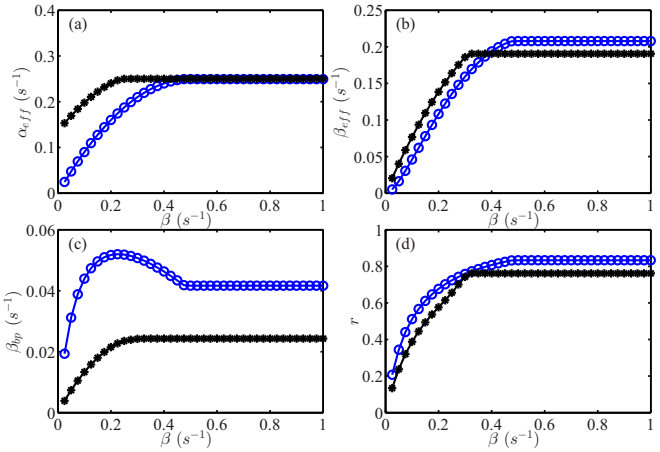

FIG. 5. (Color online) The effective transcription initiation rate α_{eff} (a), effective transcription rate β_{eff} (b), bypass transcription rate β_{bp} (c), and transcription effectiveness r (d) as functions of the termination rate β. The lines with marker "$\circ$" are obtained with zero detachment rate k_d but nonzero backtracking rate k_b, while the lines with marker "$*$" are obtained with nonzero detachment rate k_d but zero backtracking rate k_b. In calculations, the termination rate β changes from 0.025 to 1 with an increment of 0.025; for other parameter values, see Table II.

approach one limit value. In the calculations of Fig. 4(a), the line with marker "$*$" is obtained with large termination rate β and nonzero detachment rate k_d, the line with marker "$\circ$" is obtained with small termination rate β and nonzero detachment rate k_d, and the thick solid line is obtained with small termination rate β and zero detachment rate. Thus, the plots in Fig. 4(a) also imply that the initiation rate limit of the effective rate α_{eff} increases with the termination rate β and detachment rate k_d. For large initiation rate α, the effective transcription rate β_{eff} also has one limit value, which increases with termination rate β and detachment rate k_d; see Fig. 4(b). However, different with the effective initiation rate α_{eff}, β_{eff} may not change monotonically with initiation rate α. The plots in Fig. 4(c) show that the bypass transcription rate β_{bp} increases with the initiation rate α and tends to one limit value when α is large enough. The limit value of β_{bp} increases with termination rate β but decreases with detachment rate k_d. This is because, for large values of detachment rate k_d, polymerase will have less chance to reach the stop site of the template. Finally, the transcription effectiveness r decreases with initiation rate α, and its limit value increases with both the termination rate β and detachment rate k_d; see Fig. 4(d).

Except for the bypass transcription rate β_{bp}, both of the rates α_{eff} and β_{eff} and the effectiveness r increase monotonically with the termination rate β and tend to approach corresponding limit values for large β; see Fig. 5. The backtracking of stalled polymerase at damaged site l can help to raise the transcription effectiveness r [see the line with marker "$\circ$" in Fig. 5(d)]. For high termination rate β, $\beta > 0.5$, backtracking also helps to raise the effective transcription rate β_{eff} [see the plots in Fig. 5(b)]. Therefore, high termination rate and backtracking rate are beneficial to getting a high effective transcription rate and to increasing the transcription effectiveness. With backtracking but no detachment, the stalled polymerase at damaged site l will have additional chance to continue its transcription.

Without detachment, i.e., $k_d = 0$, there are only two mechanisms for the stalled polymerase to leave damaged site l, backtracking to site $l-1$ and waiting for the repair of site l or bypassing the damaged site l and continuing its transcription from site $l+1$. With the increase of backtracking rate k_b, the translocation of polymerase along the template will be slowed down. Thus, the effective transcription initiation rate α_{eff} decreases with backtracking rate k_b; see Fig. 6(a). Given that there are only two mechanisms for the stalled polymerase to leave damaged site l, the increase of backtracking rate will lead to the decrease of the probability of bypass. This implies that the bypass transcription rate decreases with backtracking rate k_b; see Fig. 6(c). Finally, the plots in Figs. 6(b) and 6(d) show that both the effective transcription rate β_{eff} and the transcription effectiveness r increase with backtracking rate k_b. Thus, backtracking is one of the ideal mechanisms for cells to solve the stalling problem.

If the stalled polymerase can only continue its translocation by the bypass mechanism, i.e., bypass the damaged site l and continue its transcription from site $l+1$, and cannot backtrack to site $l+1$ or detach from the template, then the effective transcription initiation rate α_{eff}, the bypass transcription rate β_{bp}, and the effective transcription rate β_{eff} will all increase with the bypass rate b_{bp}; see Figs. 7(a)–7(c). The increase of rate β_{eff} with bypass rate b_{bp} is because, with large values of k_{bp}, the polymerase with correctly synthesized mRNA

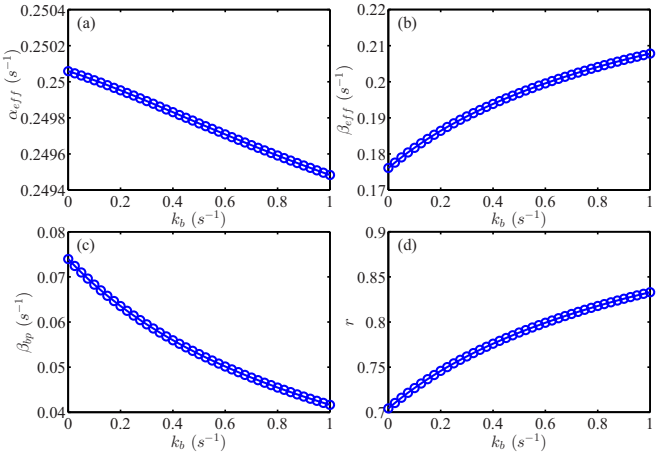

FIG. 6. (Color online) The effective transcription initiation rate α_{eff} (a), effective transcription rate β_{eff} (b), bypass transcription rate β_{bp} (c), transcription effectiveness r (d) as functions of the backtracking rate k_b. In calculations, k_b changes from 0 to 1 with an increment of 0.025. The detachment rate k_d is set to zero; i.e., stalled polymerases at damaged site l will not detach from the template. Other parameter values used in calculations are listed in Table II.

will have less possibility to be blocked during its transcription process. However, the plots in Fig. 7(d) indicate that transcription effectiveness r decreases with bypass rate k_{bp}. Besides the bypass mechanism, if the stalled polymerase can also backtrack to the previous site $l-1$ to wait for the repair of the damaged site l, then the rates α_{eff} and β_{eff} and effectiveness r will be increased [see the lines with markers "$\circ$" and "$*$" in Figs. 7(a), 7(b), and 7(d)]. The lines plotted in Fig. 7(c) with markers "$\circ$" and "$*$" show that, with additional

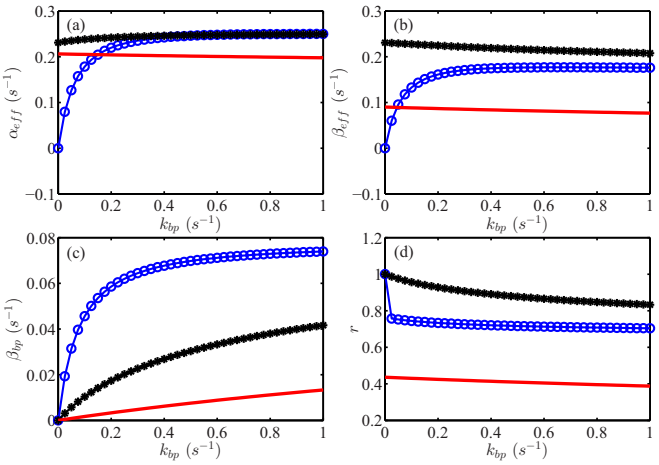

FIG. 7. (Color online) The effective transcription initiation rate α_{eff} (a), effective transcription rate β_{eff} (b), bypass transcription rate β_{bp} (c), and the transcription effectiveness r (d) as functions of the bypass rate k_{bp}. In each figure, three typical examples are plotted, where the lines with marker "$*$" are obtained with $k_d = 0$ and $k_b \neq 0$, the thick solid lines are obtained with $k_d \neq 0$ and $k_b = 0$, and the lines with marker "$\circ$" are obtained with $k_d = k_b = 0$. The bypass rate k_{bp} changes from 0 to 1 with an increment of 0.025. The values of other parameters are listed in Table II.

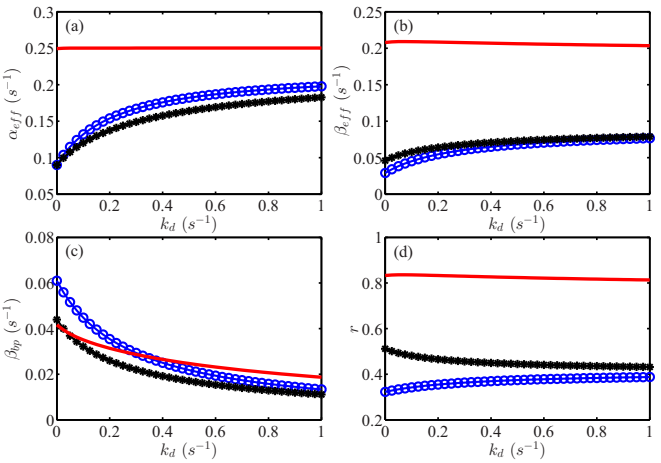

FIG. 8. (Color online) The effective transcription initiation rate α_{eff} (a), effective termination rate β_{eff} (b), bypass transcription rate β_{bp} (c), and the transcription effectiveness r (d) as functions of the detachment rate k_d. The lines with marker "$\circ$" are for the cases with zero backtracking rate k_b, and the thick solid lines are calculated with large transcription termination rate β. In all calculations, the detachment rate k_d changes from 0 to 1 with an increment of 0.025. For other parameter values used in calculations, see Table II.

backtracking mechanism, i.e., $k_b \neq 0$, the bypass transcription rate β_{bp} will be reduced. Meanwhile, all the solid lines and the lines with marker "$\circ$" in Figs. 7(a)–7(d) show that with additional detachment mechanism, i.e., $k_d \neq 0$, all the effective rates α_{eff}, β_{eff}, and β_{bp} and the transcription effectiveness r will be reduced. This implies that the detachment of stalled polymerase may not be a good mechanism for cells to solve the transcription stalling problem and to increase their transcription rate and efficiency. The plots in Fig. 7 also show that, for the special cases with either nonzero detachment rate or nonzero backtracking rate, the effective rates α_{eff}, β_{eff}, and β_{bp} only change slightly with the bypass rate k_{bp}.

The plots in Fig. 8(a) show that, generally, the effective initiation rate α_{eff} increases with the detachment rate of stalled polymerase at damaged site l. Because for large values of detachment rate, the polymerase density between site 0 and site l will be low. Therefore, the effective initiation rate $\alpha_{\text{eff}} = \alpha(1-p_0)$ will be large. However, for the cases with large termination rate β, α_{eff} is almost independent of detachment rate k_d; see the thick solid line in Fig. 8(a). This is because, for large termination rate β, the polymerase density along transcription template is low enough, and the influence of detachment of stalled polymerase can be neglected. In other words, detachment will not help to reduce the polymerase density any longer. From the plots in Fig. 8(b), one can see that for low termination rate β, the effective transcription rate β_{eff} increases with detachment rate k_d. The reason is that large detachment rate k_d will be helpful to reduce the polymerase density along the transcript template. Consequently, the mean translocation speed of polymerase will be high. However, for large values of termination rate β, β_{eff} decreases with detachment rate k_d [see the thick solid line in Fig. 8(b)]. Given large values of β, the polymerase density along template

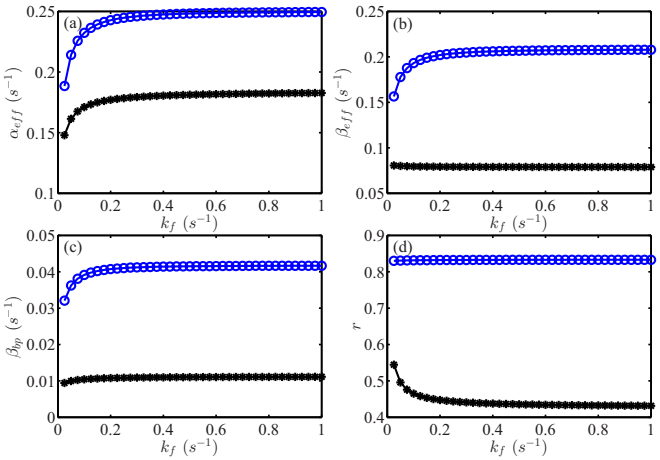

FIG. 9. (Color online) The effective transcription initiation rate α_{eff} (a), effective termination rate β_{eff} (b), bypass termination rate β_{bp} (c), and the transcription effectiveness r (d) as functions of the forward rate k_f [see Fig. 1(a) for the meaning of k_f]. The lines with marker "$\circ$" are obtained with zero detachment rate k_d and high termination rate β, while the lines with marker "$*$" are obtained with nonzero detachment rate k_d and low termination rate β. In all calculations, the forward rate k_f changes from 0.025 to 1 with an increment of 0.025. The values of other parameters are listed in Table II.

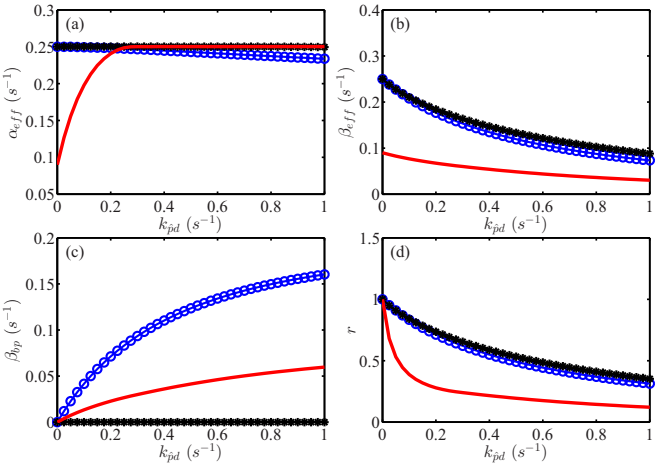

FIG. 10. (Color online) The effective transcription initiation rate α_{eff} (a), effective termination rate β_{eff} (b), bypass termination rate β_{bp} (c), and the transcription effectiveness r (d) as functions of the damage rate $k_{\hat{p}d}$. The lines with marker "$\circ$" are obtained with zero detachment rate k_d, the lines with marker "$*$" are obtained with zero bypass rate k_{bp}, and the thick solid lines are obtained with zero backtracking rate k_b and low termination rate β. In all calculations, the damage rate $k_{\hat{p}d}$ changes from 0 to 1 with an increment of 0.025. The values of other parameters are listed in Table II.

will be low enough that each polymerase can translocate forward freely. Thus, with large values of detachment rate k_d, polymerase will have less opportunity to complete its whole transcription process. This means that the effective transcription rate β_{eff} will be low for large detachment rate k_d. Because there are altogether three possible mechanisms for stalled polymerase to leave the damaged site l, i.e., backtracking, detachment, and bypass, the bypass transcription rate β_{bp} will be low for large detachment rate k_d; see Fig. 8(c). The plots in Fig. 8(d) show that, for the cases with nonzero backtracking rate k_b, transcription effectiveness r decreases slightly with detachment rate k_d. However, for the cases with zero backtracking rate, effectiveness r increases with k_d. This implies that when there is no backtracking, detachment is a good mechanism to solve the polymerase stalling problem. Generally, however, backtracking may be better than detachment at increasing the transcription efficiency.

Figures 9(a)–9(c) show that all the effective rates, α_{eff}, β_{eff}, and β_{bp} increase with the return back rate k_f of the backtracked polymerase, since large value of rate k_f means that the backtracked polymerase at site $l-1$ will return back to site l quickly when the damaged site l has been repaired, and then restart its transcription. However, the plots in Fig. 9(d) show that for nonzero detachment rate k_d and low termination rate β, transcription effectiveness decreases with rate k_f. Given low termination rate β, the polymerase density between sites l and N will be high, so the increase of return back rate k_f has little influence to increase the effective transcription rate β_{eff} [see the line in Fig. 9(b) with marker "$*$"]. However, for nonzero detachment rate k_d, the polymerase translocation between sites 0 and l may be uncrowded; thus, the effective transcription initiation rate α_{eff} increases with the return back rate k_f [see the line in Fig. 9(a) with marker "$*$"]. Therefore, from the definition of transcription effectiveness, $r := \beta_{\text{eff}}/\alpha_{\text{eff}}$, for the cases with low termination rate β but nonzero detachment rate k_d, transcription effectiveness r decreases with the return back rate k_f. Therefore, large return back rate k_f may not be helpful to increase the efficiency of transcription.

Finally, the plots in Figs. 10(b)–10(d) show that the effective transcription rate β_{eff} and transcription effectiveness r decrease with the damage rate $k_{\hat{p}d}$ of site l, while the bypass transcription rate β_{bp} increases with $k_{\hat{p}d}$. For high damage rate $k_{\hat{p}d}$, the polymerase is more likely to be stalled at the site l, and then the possibility of bypass will be high and the synthesis speed of correct mRNA will be low. The plots in Fig. 10(a) imply that, for low termination rate β and low backtracking rate k_b, the effective initiation rate α_{eff} increases with damage rate $k_{\hat{p}d}$. Given low termination rate β, the polymerase density along transcription template will be high and the translocation speed of polymerase will be low. With the increase of damage rate $k_{\hat{p}d}$, the stalled polymerase will have more possibility to detach from the template. So the total leaving rate of polymerase from the transcription template, either from the stop site N or from the damaged site l, will increase. Thus, the effective initiation rate α_{eff} increases with the damage rate $k_{\hat{p}d}$. The line with marker "$\circ$" in Fig. 10(a) also show that, without detachment, the effective initiation rate α_{eff} decreases with damage rate $k_{\hat{p}d}$. This is because, for a large damage rate, polymerase will be more likely to be stalled at the damaged site l and, consequently, the translocation speed of polymerase along transcription template will be slowed down.

Although previous results show that backtracking mechanism maybe the best choice for stalled polymerase to continue its transcription process, bypass and degradation are also necessary. The plots in Fig. 11 show that there is a tradeoff between rates $k_{bp} = k_d$ and rate k_b. With large backtracking rate k_b but small degradation and bypass rates

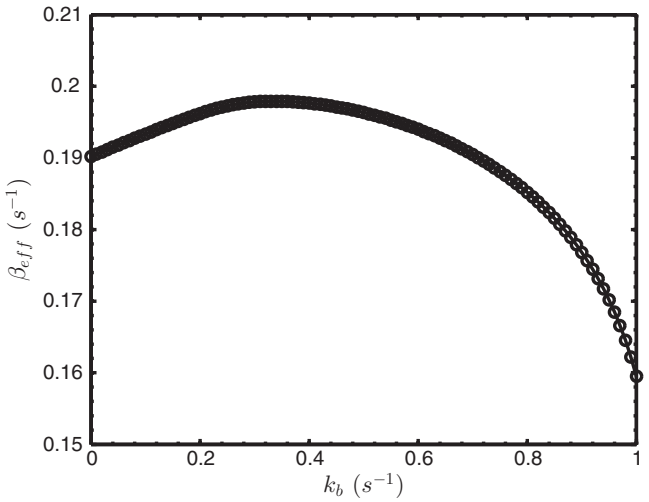

FIG. 11. The change of effective rate β_{eff} as a function of backtracking rate k_b, for special parameter values $N = 200, l = 100$, $\alpha = \beta = k_E = k_{\hat{p}r} = 1$, $k_f = k_{\hat{p}d} = 0.1$, and k_b, k_{bp}, and k_d satisfy $k_b + k_{bp} + k_d = 1$, $k_{bp} = k_d$. This plot implies that degradation mechanism and bypass mechanism are also helpful to improve the effective transcription rate, which cannot be replaced by the backtracking mechanism.

k_{bp} and k_d, the effective rate β_{eff} decreases with backtracking rate k_b. On the contrary, for large values of k_{bp} and k_d, i.e., small values of backtracking rate k_b, the effective rate β_{eff} increases with k_b, which means that bypass mechanism and degradation mechanism cannot be replaced by the backtracking.

IV. CONCLUDING REMARKS

In this study, a modified TASEP model is presented to describe gene transcription process including polymerase stalling. Because of the detachment (or degradation) of polymerase from the damaged site, the polymerase density along transcription template has a sharp change at the damaged site. As in usual TASEP models, the polymerase density may have boundary layers at the transcription start site and termination site. In the main body of the transcription template, the polymerase density may be in three phases: low density phase, high density phase, and maximal flux phase. However, the phases in different regions of the transcription template may be different. This study showed that the effective transcription rate (the rate to synthesize mRNA correctly) and the transcription effectiveness (the proportion of correct transcription) will be high if the damaged site of the transcription template is close to the transcription termination site. The increase of transcription initiation rate will increase the effective transcription rate but decrease the transcription effectiveness. On the other hand, the increase of transcription termination rate will increase the effective transcription rate and the transcription effectiveness, as well as the effective transcription initiation rate.

Experiments found that there are three mechanisms for cells to solve the polymerase stalling problem: backtracking, bypass, and detachment. This study showed that the increase of backtracking rate will lead to the increase of effective transcription rate and the transcription effectiveness, but lead to the decrease of the effective transcription initiation rate. It implies that backtracking is one of the ideal mechanisms to increase the synthesizing rate of mRNA and the transcription efficiency. Without backtracking and detachment, the increase of bypass rate will lead to the increase of effective transcription rate. However, for general cases, large values of bypass rate will lead to low values of effective transcription rate and the transcription effectiveness. Similarly, without backtracking, detachment (or degradation) of the stalled polymerase is a good mechanism to solve the stalling problem. However, for nonzero backtracking rate cases, the increase of detachment rate may lead to the decrease of effective transcription rate and transcription effectiveness. As expected, the increase of damage rate of the transcription template will lead to the decrease of transcription efficiency.

The results obtained in this study will be helpful in understanding gene transcription in living cells and the mechanisms used by cells to solve the polymerase stalling problem. The model presented in this study can be further generalized to discuss more general cases of gene transcription process in which polymerase may be stalled at more than one site of the transcription template. The model parameter values in real cells may be extracted through the NET-seq approach presented in [39], and then the theoretical model given in this study can be used to do quantitative analysis of the gene transcription process with polymerase stalling. Finally, combining this study with the recent model presented by Choubey *et al.* in [40], more details of the transcript process can be better understood.

ACKNOWLEDGMENTS

This study was supported by the Natural Science Foundation of China (Grant No. 11271083) and the National Basic Research Program of China (National "973" program, Project No. 2011CBA00804).

[1] J. Krug, Boundary-induced phase transitions in driven diffusive systems, Phys. Rev. Lett. **67**, 1882 (1991).
[2] B. Derrida, S. A. Janowsky, J. L. Lebowitz, and E. R. Speer, Exact solution of the totally asymmetric simple exclusion process: Shock profiles, J. Stat. Phys. **73**, 813 (1993).
[3] B. Derrida, M. R. Evans, V. Hakim, and V. Pasquier, Exact solution of a 1D asymmetric exclusion model using a matrix formulation, J. Phys A: Math. Gen. **26**, 1493 (1993).
[4] G. Schutz and E. Domany, Phase transitions in an exactly soluble one-dimensional exclusion process, J. Stat. Phys. **72**, 277 (1993).
[5] A. Kolomeisky, G. M. Schutz, E. B. Kolomeisky, and J. P. Straley, Phase diagram of one-dimensional driven lattice gases with open boundaries, J. Phys. A: Math. Gen. **31**, 6911 (1998).
[6] Y. Zhang, Periodic one-dimensional hopping model with transitions between nonadjacent states, Phys. Rev. E **84**, 031104 (2011).

[7] Y. Zhang, Theoretical analysis of kinesin KIF1A transport along microtubule, J. Stat. Phys. **152**, 1207 (2013).
[8] A. Azvolinsky, P. G. Giresi, J. D. Lieb, and V. A. Zakian, Highly transcribed RNA polymerase II genes are impediments to replication fork progression in saccharomyces. Mol. Cell **34**, 722 (2009).
[9] J. Z. Dalgaard and A. J. S. Klar, A DNA replication-arrest site RTS1 regulates imprinting by determining the direction of replication at mat1 in S. pombe, Genes Dev. **15**, 2060 (2001).
[10] B. J. Brewer and W. L. Fangman, A replication fork barrier at the 3′ end of yeast ribosomal RNA genes, Cell **55**, 637 (1988).
[11] M. Gruber, R. E. Wellinger, and J. M. Sogo, Architecture of the replication fork stalled at the 3′ end of yeast ribosomal genes, Mol. Cell. Biol. **20**, 5777 (2000).
[12] T. Nouspikel and P. C. Hanawalt, DNA repair in terminally differentiated cells, DNA Repair **1**, 59 (2002).
[13] A. M. Casper, P. Nghiem, M. F. Arlt, and T. W. Glover, ATR regulates fragile site stability, Cell **111**, 779 (2002).
[14] R. S. Cha and N. Kleckner, ATR homolog Mec1 promotes fork progression, thus averting breaks in replication slow zones, Science **297**, 602 (2002).
[15] A. Daraba, V. K. Gali, M. Halmai, L. Haracska, and I. Unk, Def1 promotes the degradation of Pol3 for polymerase exchange to occur during DNA-damage–induced mutagenesis in saccharomyces cerevisiae, PLoS Biol. **12**, e1001771 (2014).
[16] G. E. Damsma, A. Alt, F. Brueckner, T. Carell, and P. Cramer, Mechanism of transcriptional stalling at cisplatin-damaged DNA, Nat. Struct. Mol. Biol. **14**, 1127 (2007).
[17] C. Walmacq, A. C. M. Cheung, M. L. Kireeva, L. Lubkowska, C. Ye, D. Gotte, J. N. Strathern, T. Carell, P. Cramer, and M. Kashlev, Mechanism of translesion transcription by RNA polymerase II and its role in cellular resistance to DNA damage, Mol. Cell **46**, 18 (2012).
[18] E. R. Edenberg, M. Downey, and D. Toczyski, Polymerase stalling during replication, transcription and translation, Curr. Biol. **24**, R445 (2014).
[19] M. Giannattasio, F. Lazzaro, M. P. Longhese, P. Plevani, and M. Muzi-Falconi, Physical and functional interactions between nucleotide excision repair and DNA damage checkpoint, EMBO J. **23**, 429 (2004).
[20] A. Ciccia, A. V. Nimonkar, Y. Hu, I. Hajdu, Y. J. Achar, L. Izhar, S. A. Petit, B. Adamson, J. C. Yoon, S. C. Kowalczykowski, D. M. Livingston, L. Haracska, and S. J. Elledge, Polyubiquitinated PCNA recruits the ZRANB3 translocase to maintain genomic integrity after replication, Mol. Cell **47**, 396 (2012).
[21] R. Weston, H. Peeters, and D. Ahel, ZRANB3 is a structure-specific ATP-dependent endonuclease involved in replication stress response, Genes Dev. **26**, 1558 (2012).
[22] J. Yuan, G. Ghosal, and J. Chen, The HARP-like domain-containing protein AH2/ZRANB3 binds to PCNA and participates in cellular response to replication stress, Mol. Cell **47**, 410 (2012).
[23] W. Vermeulen and M. Fousteri, Mammalian transcription-coupled excision repair, Cold Spring Harbor Perspect. Biol. **5**, a012625 (2013).
[24] S. Lagerwerf, M. G. Vrouwe, R. M. Overmeer, M. I. Fousteri, and L. H. F. Mullenders, DNA damage response and transcription, DNA Repair **10**, 743 (2011).
[25] A. M. Deaconescu, RNA polymerase between lesion bypass and DNA repair, Cell. Mol. Life Sci. **70**, 4495 (2013).
[26] N. P. Higgins, K. Kato, and B. Strauss, A. model for replication repair in mammalian cells, J. Mol. Biol. **101**, 417 (1976).
[27] P. Stelter and H. D. Ulrich, Control of spontaneous and damage-induced mutagenesis by SUMO and ubiquitin conjugation, Nature (London) **425**, 188 (2003).
[28] K. Watanabe, S. Tateishi, M. Kawasuji, T. Tsurimoto, H. Inoue, and M. Yamaizumi, Rad18 guides polη to replication stalling sites through physical interaction and PCNA monoubiquitination, EMBO J. **23**, 3886 (2004).
[29] M. D. Wilson, M. Harreman, and J. Q. Svejstrup, Ubiquitylation and degradation of elongating RNA polymerase II: The last resort, Biochim. Biophys. Acta **1829**, 151 (2013).
[30] C. J. Shoemaker and R. Green, Translation drives mRNA quality control, Nat. Struct. Mol. Biol. **19**, 594 (2012).
[31] M. K. Doma and R. Parker, Endonucleolytic cleavage of eukaryotic mRNAs with stalls in translation elongation, Nature (London) **440**, 561 (2006).
[32] T. Becker, J.-P. Armache, A. Jarasch, A. M. Anger, E. Villa, H. Sieber, B. A. Motaal, T. Mielke, O. Berninghausen, and R. Beckmann, Structure of the no-go mRNA decay complex Dom34-Hbs1 bound to a stalled 80S ribosome, Nat. Struct. Mol. Biol. **18**, 715 (2011).
[33] C. J. Shoemaker, D. E. Eyler, and R. Green, Dom34:Hbs1 promotes subunit dissociation and peptidyl-tRNA drop-off to initiate no-go decay, Science **330**, 369 (2010).
[34] C. T. MacDonald, J. H. Gibbs, and A. C. Pipkin, Kinetics of biopolymerization on nucleic acid templates, Biopolymers **6**, 1 (1968).
[35] R. K. P. Zia, J. J. Dong, and B. Schmittmann, Modeling translation in protein synthesis with TASEP: A tutorial and recent developments, J. Stat. Phys. **144**, 405 (2011).
[36] T. Tripathi and De. Chowdhury, Interacting RNA polymerase motors on a DNA track: Effects of traffic congestion and intrinsic noise on RNA synthesis, Phys. Rev. E **77**, 011921 (2008).
[37] J. Li and Y. Zhang, Relationship between promoter sequence and its strength in gene expression, Eur. Phys. J. E **37**, 86 (2014).
[38] L. E. Maquat, Nonsense-mediated mRNA decay: Splicing, translation and mRNP dynamics, Nat. Rev. Mol. Cell Biol. **5**, 89 (2004).
[39] L. S. Churchman and J. S. Weissman, Nascent transcript sequencing visualizes transcription at nucleotide resolution, Nature (London) **469**, 368 (2011).
[40] S. Choubey, J. Kondev, and A. Sanchez, Deciphering transcriptional dynamics in vivo by counting nascent RNA molecules, arXiv:1311.0050v2.